

Short Communication

Carbon Nanotubes-Silicon Nanocomposites Based Resistive Temperature Sensors

Muhammad Tariq Saeed Chani^{1,2*}, Abdullah M. Asiri^{1,2}, Kh. S. Karimov^{3,4}, Mehran Bashir³, Sher Bahadar Khan^{1,2}, Mohammed M. Rahman^{1,2}

¹Center of Excellence for Advanced Materials Research (CEAMR), King Abdulaziz University, Jeddah 21589, P.O. Box 80203, Saudi Arabia

²Department of Chemistry, Faculty of Science, King Abdulaziz University, Jeddah 21589, P.O. Box 80203, Saudi Arabia

³GIK Institute of Engineering Sciences and Technology, Topi 23640, Swabi, Pakistan.

⁴Physical Technical Institute of Academy of Sciences, Rudaki Ave.33, Dushanbe, 734025, Tajikistan.

*E-mail: tariqchani@hotmail.com, tariqchani1@gmail.com

Received: 24 August 2014 / Accepted: 11 January 2014 / Published: 23 March 2015

This work presents the fabrication and temperature sensing properties of the carbon nanotubes-silicon (CNT-Si) nanocomposites based sensors. The multi-walled carbon nanotubes used for the fabrication of sensors have diameter in the range of 10-30, while the silicon powder (1.99 μm) is obtained by the milling of p-Si crystal wafers containing impurity (boron) concentration of 10^{16} cm^{-3} . For the synthesis of nanocomposites the silicone adhesive (Hero Gum) and organic polymer (GMSA) are used as a binding materials. Four different types of composites are prepared for the fabrication of sensors. Film deposition is carried out by using drop casting and doctor blade technology. In all the sensors entire thickness of composite film is equal to 100 μm . The temperature sensitivity is found in the range of -0.53 %/ $^{\circ}\text{C}$ to -0.74 %/ $^{\circ}\text{C}$. Depending on composition, ratio of components and kind of adhesive materials the initial resistance values of the sensors are in the range of 260 Ω to 34 k Ω . The simulation of experimental results is carried out by using exponential function and the simulated results are in good agreement with the experimental results.

Keywords: Carbon nanotubes; Temperature sensing; Simulation; Nanocomposites

1. INTRODUCTION

Although, existence of cementite nanowires and CNTs in some antique engineering products has been proved recently [1], but the discovery of CNTs by Iijima in 1991 [2, 3] brought a revolution in the world of scientific research and it has become the most investigated material of 20th century. It

all is because of its exceptional mechanical, thermal and electronic properties [4]. Depending on the chirality of the tube, carbon nanotubes are electronically categorized as semiconducting (wide or small bandgap) and metallic [4, 5]. The CNTs in the form of single-walled, double-walled and multi-walled tubes have been studied as an active material for various types of sensors [3, 6-14]. Because of their piezoresistive nature, CNTs are interesting for electromechanical sensors like accelerometer, pressure sensors, displacement sensors and strain sensors. Due to their temperature dependent resistivity carbon nano tubes are also considered very promising active material for temperature sensors [15], that can offer extensive miniaturization, low power consumption, high sensitivity and quick response [16, 17]. These sensors may be used in MEMS, medical, agriculture, food, chemical, mechanical, nuclear and aerospace industries.

Volder et al. fabricated low power consuming miniaturized temperature sensors by growing 3D bridge of CNTs on TiN electrodes by using Ni as a catalyst, while silicon wafer is used as a substrate [17]. The reported sensitivity of the these sensors between 300K and 420K is 0.1 %/K. Ali et al. reported the controlled growth of CNTs on silicon (Si (100)) substrate by using yttrium iron alloy as a catalyst and they tested the samples for temperature sensing [18]. The reported sensitivity is $4.21 \times 10^{-4} \text{ } ^\circ\text{C}^{-1}$ with ultrafast response. Karimov et al. reported the fabrication of CNTs based sensors on a paper substrate by the sequential deposition of glue and multi walled carbon nanotubes films, which show sensitivity of $-0.24\%/^\circ\text{C}$ [19]. These sensors are fabricated by deposition of 30-40 μm thick CNTs films, while the sensors width and inter-electrodes distances are 4 and 5 mm respectively. A carbon nano-wires array on a diamond substrate is fabricated by using focused ion beam (30 KeV Ga^+) for temperature sensing in the range of 40-140 $^\circ\text{C}$ by Zaitsev et al. [20]. The sensing mechanism is based on change in current with change in temperature. Semiconducting CNTs grown by ion beam deposition method on nickel film is characterized for low temperature sensing by Saraiya et al. [21]. The current study is focused on temperature sensing properties of CNTs and CNTs-Si based composites.

2. EXPERIMENTAL

For the fabrication of sensors commercially produced (Sun Nanotech Co Ltd., China) CNTs powder is used. The diameter of multiwalled carbon nanotubes (MWNTs) varies between 10-30 nm. The silicon powder is obtained by the milling of p-Si crystal wafer, which with has 10^{16} cm^{-3} impurity (boron) concentration. Average size of the particles in silicone powder is equal to 1.99 μm that is found by particle size analyzer SA-CP 3. As adhesive materials the Hero Gum (silicone adhesive) and GMSA (organic polymer) are used. The composites are obtained by mixing the components. The medical glass slides are used as substrate, which are cleaned and dried prior to the deposition of blends. Four different types of sample are prepared by the sequential use of drop casting and doctor blade technology. The composition and the dimensions of the composite films are given in Table-1. Figure 1 (a) and (b) show schematic diagrams of the samples 1-3, and 4 respectively. The thickness of active films is equal to 100 μm in both single (1-3) and bi-layer sensors (4). In bi-layer structure the thickness of p-Si-adhesive and CNT-adhesive composites are equal to 80 μm and 20 μm , respectively

(layer-1 and layer-2 in Fig.1 (b)). Terminals of the sensors are connected to the composites layers by the silver paste. After fabrication, the samples are dried for two days at room temperature conditions followed by heating at 90 °C for two hrs by using hot-plate. The resistance and temperature are measured by FLUKE 87multi-meter.

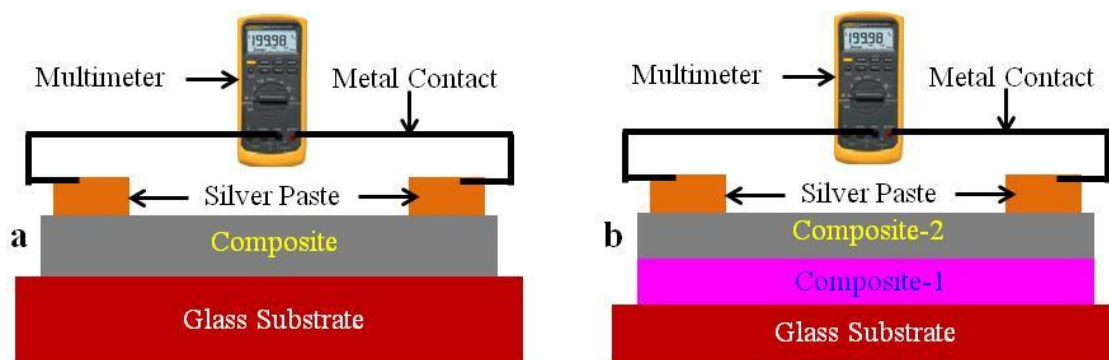


Figure 1. Schematic diagrams of the sensors

3. RESULTS AND DISCUSSION

Resistance-temperature relationships of the sensors are shown in Figs. 2(a)-3(b). It is evident from the figures that the DC resistance of the sensors decreases with increase in temperature. This decrease in resistance is in the range of 12% to 29%. The initial resistance values of the sensors are in the range of 263 Ω to 34 k Ω , depending of composition, ratio of components and kind of adhesive material. The sensors based on nanocomposites of CNTs-GMSA and CNTs-Herogum show low initial resistance, while the sensors based on CNTs-Si-Herogum nanocomposites show high resistance. The addition of p-Si causes to increases the initial resistances of the sensors from 662 Ω (3:7 CNT-Herogum nanocomposite) to 34 k Ω (2:4:4 CNT-p-Si-Herogum nanocomposite). The reasons behind this behavior may be the high resistance of the Si as compared to CNTs (a) and the possible formation of hetero-junctions between Si and CNTs (b). It is evident from the resistance temperature behaviors of the sensors that the sensors based on double layer of composite (Fig.3(b)) show more linear behavior as compared to the sensors based on single layer of composite (Figs.2(a) to 3(b)). It also depicts that the properties of the sensors can be easily changed by changing the composition, ratio of components in the composite and the design of sensor. For the calculation of resistance-temperature coefficient (S) following equation is used:

$$S = \frac{\Delta R}{R_o \Delta T} 100 \quad (1)$$

where R_o initial resistance, ΔR is change in resistance and ΔT is change in temperature. It is found that the sensors have sensitivity in the range of -0.53 %/°C to -0.74 %/°C, which is far more better than the sensitivities of hydrogenated multiwalled CNTs (-0.16%/°C⁻¹) [22], CNTs based micro-bridge sensors (-0.1 %/K) [17], flexible temperature sensor based on carbon-polymer composite (-0.13%K⁻¹) [20], CNTs grown on silicon substrate by using Ye-Fe catalyst (4.21 x 10⁻⁴ °C⁻¹) [18] and

the temperature sensors based on CNTs glued film on paper substrates ($-0.24\% \text{ } ^\circ\text{C}^{-1}$) [19]. More over the obtained sensitivities are also better than the sensitivity of the platinum based resistance temperature detectors, which is reported as $+0.35 \text{ } \%/^\circ\text{C}$ [23]. It reveals that in the sensor's performance, composition and film processing technology play very important role. Table-1 shows the sizes, compositions and the electrical parameters of CNT and p-Si based resistive temperature sensors.

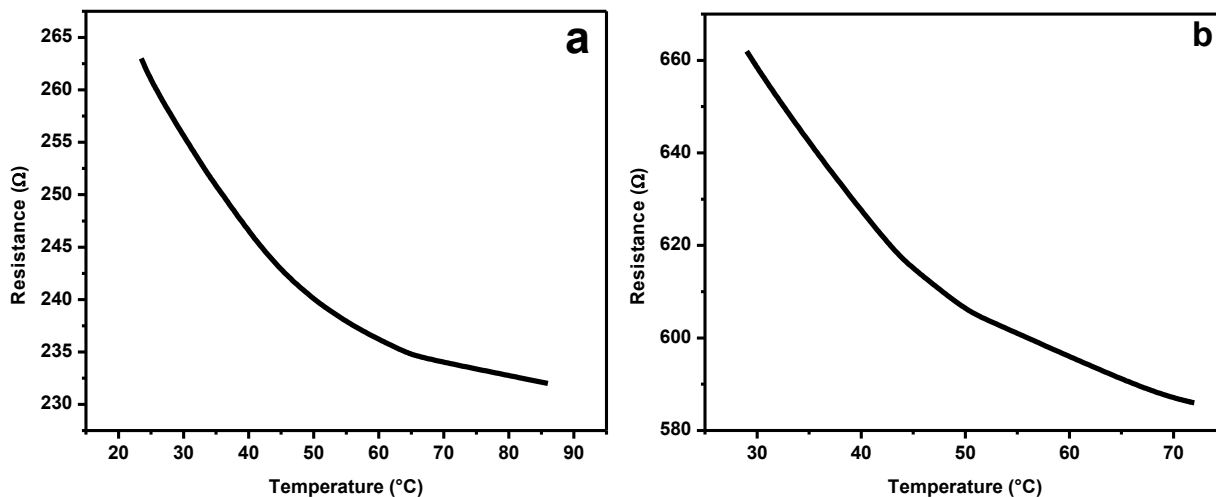


Figure 2. Resistance-temperature behavior of CNT-GMSA (a) CNT-Hero-gum (b) nanocomposite based sensor

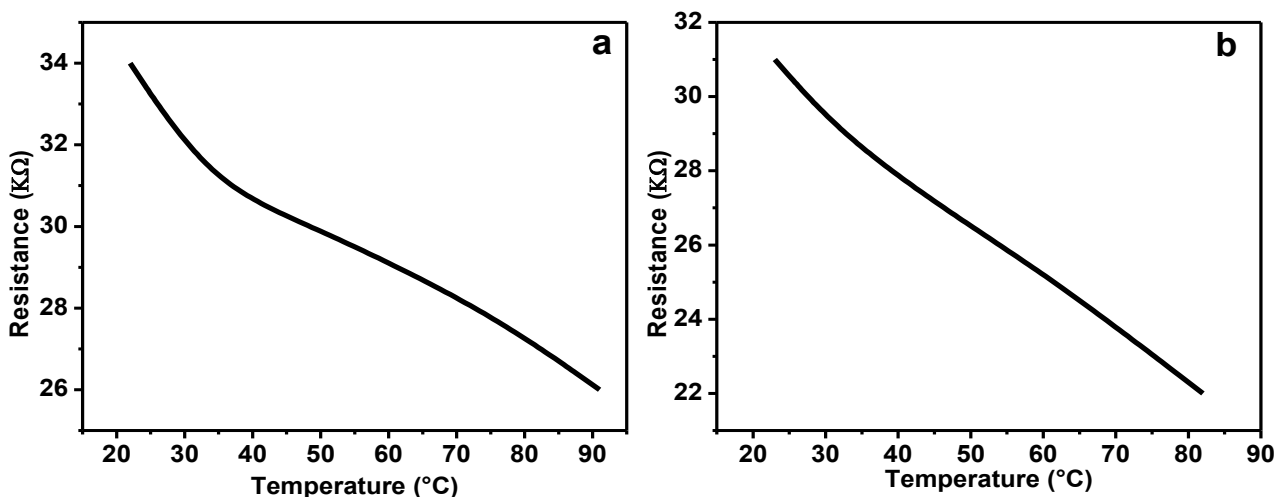


Figure 3. Resistance-temperature behavior of CNT-p-Si-Hero-gum (a) double layers (b) nanocomposite based sensor

The resistance (R) of the sensor can also be determined as [24]:

$$R = \frac{d\rho}{A} = \frac{d}{\sigma A} \tag{2}$$

where d and A are the inter-electrode distance or length and cross-section of the active layer (composite) respectively, while ρ is composite layer's resistivity ($\rho = 1/\sigma$, and σ is the conductivity). The resistance-temperature relationships shown in Figs. 2(a)-3(b) reveal that the conductivity of all p-Si and CNT composites films increases with increase in temperature, which is regarded to the increase in charge carrier concentration. The behavior of CNTs under the effect of temperature is exactly like other semiconductors [25]. The simulation of experimental data is carried out by using the exponential function shown in Eq. 3 [26].

$$f(x) = e^{-x} \tag{3}$$

Table 1. Electric parameters and composites compositions of the CNT and p-Si based resistive temperature sensors

No.	Size			R_o (Ω)	S ($\%^\circ\text{C}^{-1}$)	σ ($\Omega^{-1}\text{cm}^{-1}$)	Composition (wt.%)			
	L (mm)	W (mm)	T (μm)				GMSA	CNT	Hero Gum	p-Si
1	45	10	100	263	-0.54	1.7	50	50	-----	-----
2	40	15	100	662	-0.53	0.68	-----	30	70	-----
3	40	15	100	34×10^3	-0.74	7.8×10^{-3}	-----	20	40	40
4	30	15	100	31×10^3	-0.72	6.4×10^{-3}	Layer-1 Layer-2	30	50 70	50

For CNT-GMSA and CNT-Hero-gum nanocomposite based sensors, the above relationship is modified as given in the Eq. 4.

$$\frac{R}{R_o} = e^{-\Delta T (T_m/T) K_1} \tag{4}$$

where R_o and R are resistances at initial and elevated temperatures (T), respectively, while ΔT and T_m are change in temperature and maximum temperature. The K_1 is the resistance temperature factor and its value is $2.0 \times 10^{-3} \text{ }^\circ\text{C}^{-1}$ and $2.8 \times 10^{-3} \text{ }^\circ\text{C}^{-1}$ for CNT-GMSA and CNT-Hero-gum nanocomposite based sensors respectively. The exponential function is also modified for CNT-p-Si-silicon adhesive nanocomposite based sensors and for layered structured sensors as follows:

$$\frac{R}{R_o} = e^{-\Delta T K_2} \tag{5}$$

In above equation K_2 is a resistance temperature factor. The value of K_2 is $3.9 \times 10^{-3} \text{ }^\circ\text{C}^{-1}$ and $5.8 \times 10^{-3} \text{ }^\circ\text{C}^{-1}$ respectively, for CNT-p-Si-silicon and layered structured sensors. These values are calculated accordingly from the data presented in Fig. 3(a) and 3(b). The comparison of experimental and simulated results is shown in Figs. 4(a) to 5(b). It can be seen that simulated results are in good agreement with the experimental results.

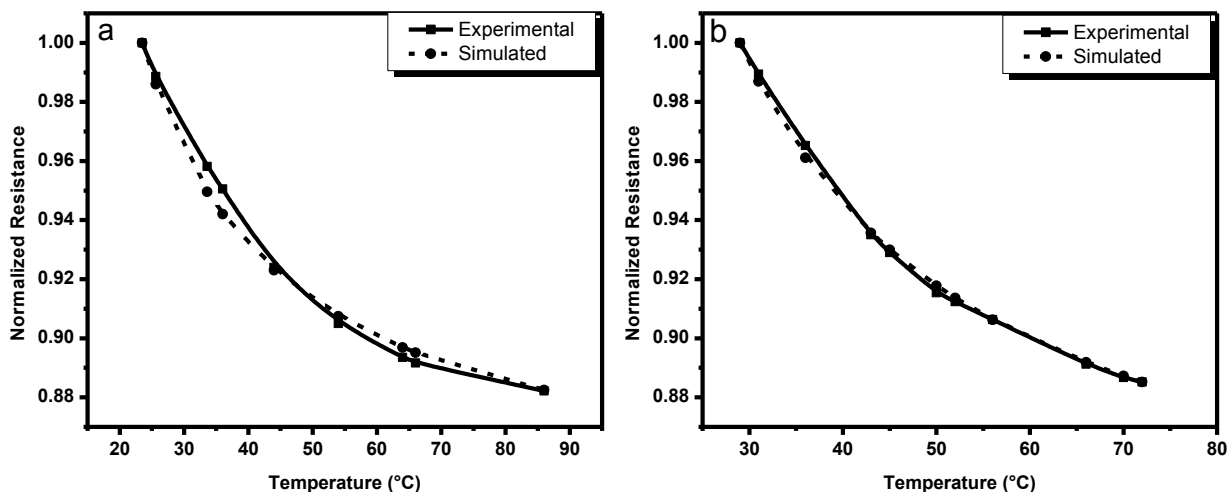


Figure 4. Comparison of experimental and simulated results of CNT-GMSA (a) CNT-Hero-gum (b) nanocomposite based sensor

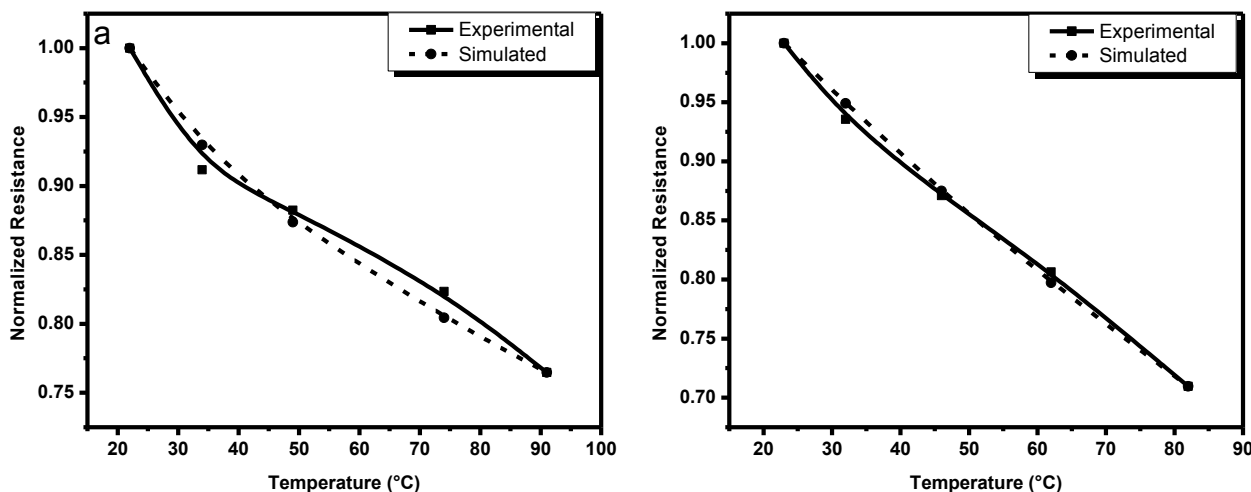


Figure 5. Comparison of experimental and simulated results of CNT-p-Si-Hero-gum (a) double layers (b) nanocomposites based sensor

The mechanism of conductivity in p-Si, CNTs and p-Si-CNTs based sensors may be considered as transitions between spatially separated sites, or particles which may be attributed to the percolation theory [27, 28]. Keeping in view the percolation theory, the effective conductivity (σ) of the composite may be calculated as

$$\sigma = \frac{1}{LZ} \tag{6}$$

where L and Z are characteristic length (it depends on sites concentration and the path resistance (having lowest average resistance), respectively). With the raise in temperature the composite layers are heated and resultantly charge carriers are generated which cause to reduce the Z . Conversely, as the semiconducting (p-Si or CNTs) powder particles are dispersed in the composite films, the squeezing of the particles may takes place because of thermal expansion. Moreover the sample's effective cross-section or the contact area between particles (Eq. 2) may also increases which may

decrease the sample's resistance. Consequently, with increase in temperature the conductivity of composite samples increases and in turn the resistance decreases, as observed in Figs. 2(a)-3(b). The composite systems may be considered as bulk hetero system which causes the high sensitivity of composite films toward the temperature effect, where the increase in inter-particles contact areas as well as the intrinsic conductivity of particles takes place; so as an outcome the conductivity of the samples increases and the resistance decreases with increase in temperature.

4. CONCLUSION

In this work the results of investigations of the electric properties of the CNT-Si nanocomposite based resistive temperature sensors are presented. By the measured resistance-temperature relationships, it is found that sensitivity of the sensors is in the range of $-0.53 \text{ \%}/^{\circ}\text{C}$ to $-0.74 \text{ \%}/^{\circ}\text{C}$, which is comparable with sensitivity of the platinum based resistance temperature detectors. Depending on the composition, ratio of components, kind of adhesive material and the design of sensor the initial values of the sensors are in the range of $263 \text{ }\Omega$ to $34 \text{ k}\Omega$. The simulated results are in good agreement with experimental results.

ACKNOWLEDGEMENTS

This paper was funded by the Deanship of Scientific Research (DSR), King Abdulaziz University (KAU), under grant No. D-004/431. The authors, therefore, acknowledge the technical and financial support of KAU.

References

1. M. Reibold, P. Paufler, A. Levin, W. Kochmann, N. Pätzke, and D. Meyer, *Nature* 444 (2006) 286-286.
2. S. Iijima, *Nature* 354 (1991) 56-58.
3. Y. Zhang, J. Liu, and C. Zhu, *Sensor Lett.* 8 (2010) 219-227.
4. K. E. Aasmundtveit, B. Q. Ta, L. Lin, E. Halvorsen, and N. Hoivik, *Journal of Micromechanics and Microengineering* 22 (2012) 074006.
5. T. W. Ebbesen, H. J. Lezec, H. Hiura, J. W. Bennett, H. F. Ghaemi, and T. Thio, *Nature* 382 (1996) 54-56.
6. C. Cantalini, L. Valentini, I. Armentano, L. Lozzi, J. Kenny, and S. Santucci, *Sensors Actuators B: Chem.* 95 (2003) 195-202.
7. K. S. Karimov, M. T. S. Chani, and F. A. Khalid, *Physica. E, low-dimensional systems and nanostructures* 43 (2011) 1701-1703.
8. K. S. Karimov, M. T. S. Chani, F. A. Khalid, A. Khan, and R. Khan, *Chinese Physics B* 21 (2012) 016102.
9. K. S. Karimov, M. T. Saeed Chani, F. Ahmad Khalid, and A. Khan, *Physica E: Low-dimensional Systems and Nanostructures* 44 (2012) 778-781.
10. P. S. Na, H. Kim, H. M. So, K. J. Kong, H. Chang, B. H. Ryu, Y. Choi, J. O. Lee, B. K. Kim, and J. J. Kim, *Appl. Phys. Lett.* 87 (2005) 093101.
11. K. Sanginovich Karimov, M. T. Saeed Chani, F. Ahmad Khalid, and A. Khan, *Physica E Low-Dimensional Systems and Nanostructures* 44 (2012) 778-781.

12. D. Tang, L. Ci, W. Zhou, and S. Xie, *Carbon* 44 (2006) 2155-2159.
13. X. Sun, X. Wang, and W. Zhao, *Sensor Lett.* 8 (2010) 247-252.
14. B. Han, X. Yu, E. Kwon, and J. Ou, *Sensor Lett.* 8 (2010) 344-348.
15. R. J. Grow, Q. Wang, J. Cao, D. Wang, and H. Dai, *Appl. Phys. Lett.* 86 (2005) 093104.
16. C. K. M. Fung, V. T. S. Wong, R. H. M. Chan, and W. J. Li, *Nanotechnology, IEEE Transactions on* 3 (2004) 395-403.
17. M. D. Volder, D. Reynaerts, C. V. Hoof, S. Tawfick, and A. J. Hart, in *IEEE Sensors Conference, IEEE, 2010*, p. 2369-2372.
18. K. Ali and M. Hafez, *Superlattices and Microstructures* 54 (2013) 1-6.
19. K. S. Karimov, M. T. S. Chani, and F. A. Khalid, *Physica E: Low-dimensional Systems and Nanostructures* 43 (2011) 1701-1703.
20. A. M. Zaitsev, A. M. Levine, and S. H. Zaidi, *physica status solidi (a)* 204 (2007) 3574-3579.
21. A. Saraiya, D. Porwal, A. Bajpai, N. Tripathi, and K. Ram, *Synthesis and Reactivity in Inorganic and Metal-Organic and Nano-Metal Chemistry* 36 (2006) 163-164.
22. V. Kumar, A. A. Bergman, A. A. Gorokhovskiy, and A. M. Zaitsev, *Carbon* 49 (2011) 1385-1394.
23. J. W. Dally, W. Riley, and K. G. McConnell, *Instrumentation for engineering measurements*, John Wiley and Sons Inc., New York, 1993.
24. M. A. Omar, *Elementary Solid State Physics: Principles and Applications*, Pearson Education (Singapore) Pt. Ltd., Indian branch, Delhi, India, 2002.
25. D. A. Neamen, *Semiconductor Physics and Devices: Basic Principles*, Richard D. Irwin Inc., Boston, USA, 1992.
26. A. Croft, T. Croft, R. Davison, and M. Hargreaves, *Engineering mathematics: a modern foundation for electronic, electrical, and control engineers*, Addison-Wesley, 1992.
27. H. Bottger and V. V. Bryksin, *Hopping conduction in solids*, Deerfield Beach, FL, 1985.
28. C. Brabec and J. P. a. N. S. V. Dyakonov, *Organic Photovoltaics: Concepts and Realization*, Springer-Verlag, Berlin Heidelberg, 2003.